SAND2017-2250J

Systematic Investigation of the Influence of Geomechanical and Hydrogeological Properties on Surface Uplift at In Salah

P. Newell[a], H. Yoon[b], J. E. Bishop[a], M. J. Martinez[a], S. L. Bryant[c]

[a] *Sandia National Laboratories, Engineering Sciences Center, Albuquerque, NM 87185 USA*

[b] *Sandia National Laboratories, Geoscience Research and Applications, Albuquerque, NM 87185 USA*

[c] *The University of Texas at Austin, Petroleum and Geosystems Engineering, Austin, TX 78712 USA*

Abstract

Coupled simulations of geological carbon storage (GCS) are important tools for understanding the long-term behavior of carbon capture and storage (CCS) systems. In this paper, we used coupled fluid flow and geomechanical numerical modeling of CO_2 storage with available field data to 1) validate our existing numerical techniques and 2) identify the key geomechanical and hydrogeological properties that impact surface uplift at In Salah. Field data includes surface deformation evaluated from data obtained from satellite-based inferometry (InSAR) as well as the maximum change in the injection-induced pore pressure. The constraint on pore pressure is the result of the bottom hole pressure being limited to remain below the fracturing gradient. These data were adapted to constrain our model. The simulation results are in good agreement with the surface uplift. However, systematic parameter variation shows the system is under constrained with available data. Several sets of parameters can fit the uplift and overpressure data equally well. The results show the pore pressure constraint is an important factor in calibrating the model. For many cases, results also reveal the vertical intrinsic permeability and Young's modulus of the reservoir remained close to 10-14 mD (1.0×10^{-14}-1.4×10^{-14} m^2) and 10 GPa, respectively. Moreover, Biot's coefficient plays an important rule in the surface uplifts and to the best knowledge of the authors, this is the only study looking at the effect of Biot's coefficient and anisotropy ratio on the surface uplift at In Salah, KB501 and KB503.

Preprint submitted to International Journal of Greenhouse Gas ControlNovember 9, 2014

Overall, this study suggests that one should be cautious in characterizing any sites or determining the operational conditions based on the limited testing data.

Keywords: Geomechanics, Geological CO_2 sequestration, In Salah, InSAR, Inverse modeling, Modeling, Mulitphysics

---

1. Introduction

Over the last decade, geologic carbon storage (GCS) has been studied to provide a promising technology to reduce CO_2 emission to the atmosphere. It is critical to understand geomechanical processes and impacts from CO_2 injection to ensure that CO_2 can be securely stored over geological times. Coupled multiphase flow and geomechanical models can be used to understand and assess effects of increased reservoir pressure by CO_2 injection on the geomechanical response. One of the prominent demonstration projects is In Salah Gas project, located in Algeria, where CO_2 recovered in natural gas production was re-injected into a sandstone reservoir formation (Eiken et al., 2011). In particular, the distribution of surface uplift was successfully evaluated using data obtained from the satellite based inferometry (InSAR) (Vasco and Novali, 2008; Vasco et al., 2008). Since then, the uplift data and other geophysical data have been used to investigate reservoir properties and coupled flow and mechanical processes (Rutqvist et al., 2009, 2010; Preisig and Prevost, 2011; Shi et al., 2013).

In the past predictions of the impact of CO_2 injection on the geomechanical response, such as surface uplift, have been performed with relatively simple models. The use of simple model is mainly because of nonlinearities of coupled multiphase flow and geomechanical response as well as associated computational expense, and/or a lack of field data. Rutqvist et al. (Rutqvist et al., 2009, 2010) investigated the relationship between the surface uplift and pore pressure change as well as deformation within the injection zone at In Salah, using coupled reservoir and geomechanical modeling. They showed consistency between the simulation results and the measured data from InSAR on the surface uplift. They demonstrated that volumetric expansion of reservoir rocks and surrounding shaly sands may attribute to the surface uplift, which depends on both permeability and elastic properties of the reservoir and overlying caprock. Preisig and Prevost (Preisig and Prevost, 2011) presented a two-dimensional (2D) fully coupled

multiphase thermo-poromechanical model for simulating CO_2 injection at In Salah. Their 2D-model over-predicted the surface uplift; they concluded the lack of the accurate data to be the reason. They also demonstrated that creation or reopening of fractures can be attributed to temperature difference between injected fluid and reservoir.

Reservoir characterization of faults and fractures has been performed to enhance the understanding of CO_2 flow in fractured rocks at In Salah (Iding and Ringrose, 2010; Pamukcu et al., 2011; Deflandre et al., 2011). Iding and Ringrose, (Iding and Ringrose, 2009, 2010) confirmed the presence of fractures and small faults in both the reservoir and the lower caprock, based on the long-term performance data of In Salah field. They concluded that despite the clear evidence of fractures in the reservoir, thick caprock layer provides an effective hydrological and mechanical barrier to CO_2 leakage. Recently, Smith et al. (Smith et al., 2011, 2013) also investigated possible fracturing within the reservoir and lower caprock near one of the CO_2 injection wells at In Salah. They concluded that at given injection rates induced fracturing into the upper caprock may not occur and the possibility of the CO_2 leakage through induced fractures is very low. In particular, geophysical inverse techniques with InSAR and seismic data were employed to estimate reservoir volume change and fault-fracture aperture change after CO_2 injection (Vasco et al., 2010). The results indicate that CO_2 associated flow can extend up to several kilometers through the fracture/fault zone in the reservoir formation at In Salah. However, all these models did not fully employ coupled multiphase flow and geomechanical modeling.

Accurate identification of geomaterial properties is essential for predicting fluid flow and geomechanical response. In reservoir engineering literature, the process of calibrating model parameters with dynamical data is known as history matching. Pamukcu et al. (Pamukcu et al., 2011) manually performed history matching to calibrate the porosity and permeability of matrix and fracture in reservoir with bottom hole pressures, CO_2 injection rates, and a CO_2 breakthrough time at a monitoring well at the In Salah site. Although predicted, using only a multiphase flow simulator, matched observed data reasonably well, they concluded that coupled multiphase flow and geomechanical modeling is required to confirm their simulation results. Recently, Shi et al. (Shi et al., 2012) performed history matching with the temporal changes in the maximum vertical uplift to estimate Young's Modulus. The reservoir model with stochastically generated porosity and permeability static fields was first calibrated with observed dynamic bottom hole pressures

to estimate fracture transimissibility of reservoir and lower caprock layers independently. Then the calibrated reservoir model was imported into coupled reservoir-geomechanical modeling in order to calibrate Young's Modulus of the lower caprock with surface uplift data near one of three injection wells (KB-501). The calibrated model was used to match InSAR surface uplifts observed at two other injection wells, demonstrating that model predictions capture the overall trend well, but the mismatch was much greater. Despite their history matching with manual tuning of 1-2 parameters, the physical models were built upon the best estimation of reservoir and geomechanical characterization. Their results clearly highlighted the importance of coupled reservoir- geomechancal modeling to evaluate the performance of CO_2 injection at the reservoir scale.

In more general aspect of reservoir simulation, Nanayakkara and Wong (Nanayakkara and Wong, 2009) gave an interesting discussion on analytical and numerical modeling of the surface uplift due to the subsurface injection. They investigated multiple cases and they showed the importance of the effect of the boundary, in terms of both the location of the boundary and the boundary conditions. Their study revealed that more realistic results could be obtained through fixed displacement boundary conditions at the bottom boundary as well as selecting sufficient lateral extent. Aoyagia et al. (Aoyagia et al., 2013) developed a numerical simulator for environmental impact assessment, which was used for In Salah CO_2 storage as a case to validate the model. They also performed a sensitivity analysis on some parameters, such as caprock permeability, porosity and Young's modulus of the reservoir. They found that caprock permeability can significantly affect the surface uplift.

Over the past decade, optimization, sensitivity, and uncertainty quantification of multiphase flow models during GCS have been developed and suggested in the literature (Espinet and Shoemaker, 2013; Wainwright et al., 2013; Tavakoli et al., 2013). In contrary, automatic parameter estimation of coupled multiphase flow and geomechanical models has not been investigated vigorously. A comparison of geomechanical deformation due to CO_2 injection highlighted the importance of systematic geomechanical evaluation prior to CO_2 injection (Verdon et al., 2013), thus there is an urgent need for further study. Furthermore, because of the non-uniqueness of the inverse problems and model uncertainty, multiple parameter sets with various starting points need to be compared. This allows evaluating the sensitivity of coupled parameters to calibrate the model (McKenna and Pike, 2013; Yoon

et al., 2013).

The aim of this study is to identify and rank the importance of key geomechanical and hydrogeological parameters using coupled flow and geomechanical simulations to have a better understanding of the surface uplift at In Salah, Algeria. Because of the lack of field data, there is a high uncertainty involved in the parameters. This uncertainty might come from geomechanical, hydrogeological properties or/and the coupling parameters. In this study, the sensitivity of the surface uplift to some of these critical parameters will be systematically investigated. Specifically, two sets of surface uplift data featuring low and high uplifts above two CO_2 injection wells are used. In addition, the maximum change of pore pressure due to CO_2 injection is included to evaluate the impact of pore pressure constraint on surface uplift during parameter estimation. After validating our coupled forward model with the representative parameter values in the literature, simulation results are used to evaluate the significance of permeability, anisotropy ratio, Young's modulus and Biot's coefficient on surface uplift and pore pressure increase. Parameter estimation with 12 different sets of parameters is performed for both KB501 and KB503. Estimated sets of parameters and resulting pore pressure calculations are used to evaluate the significance of parameterization and the inclusion of the pore pressure constraint on the geomechanical response. It should be noted that the focus is on KB501 and KB503 and all the simulations are based on these two injectors.

2. Model description

2.1. Model domain

As shown in Figure 1, In Salah gas project is located in Algeria. The simulation domain includes quarter symmetry of an injection well, and is discretized into a 3D-model 5×5×4 km. Following previous works in the literature (Rutqvist et al., 2010; Preisig and Prevost, 2011), the model consists of four distinct layers including 20 m-thick reservoir, 900 m-thick caprock layer, overlying 900 m thickness of overburden aquifer, and 2180 m-thick base aquifer (Figure 2). The supercritical CO_2 was injected via a 1000 m-long horizontal well. For simplicity, it was assumed the model domain and all conditions are identical for both the KB501 and KB503 well regions.

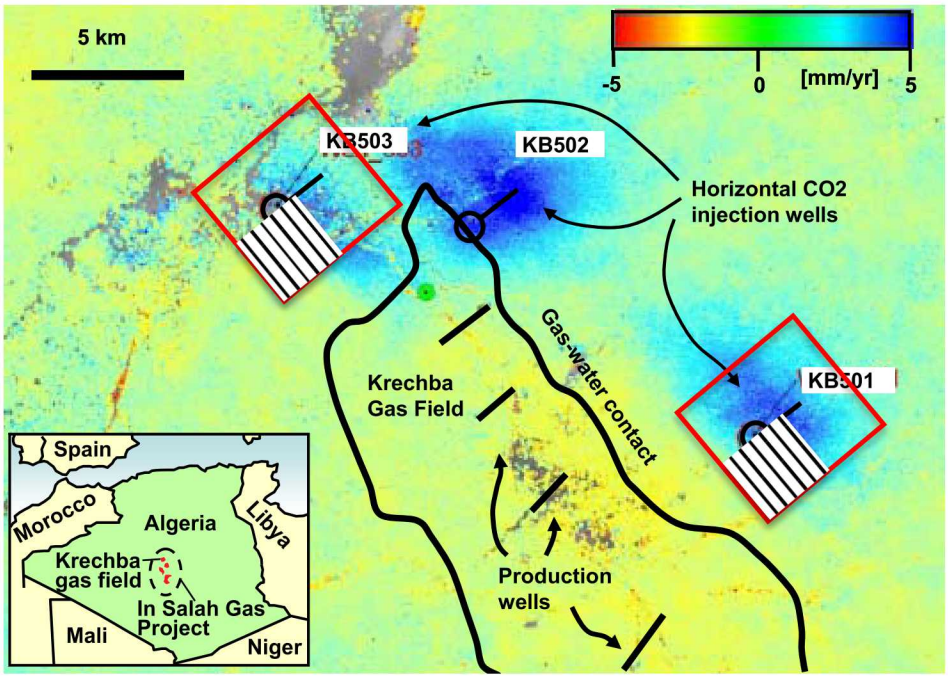

Figure 1: Krechba gas field (Rutqvist et al., 2010). The red squares show the domains for KB501 and KB503 and the dashed domains show the quarter symmetry sections being used in the simulation.

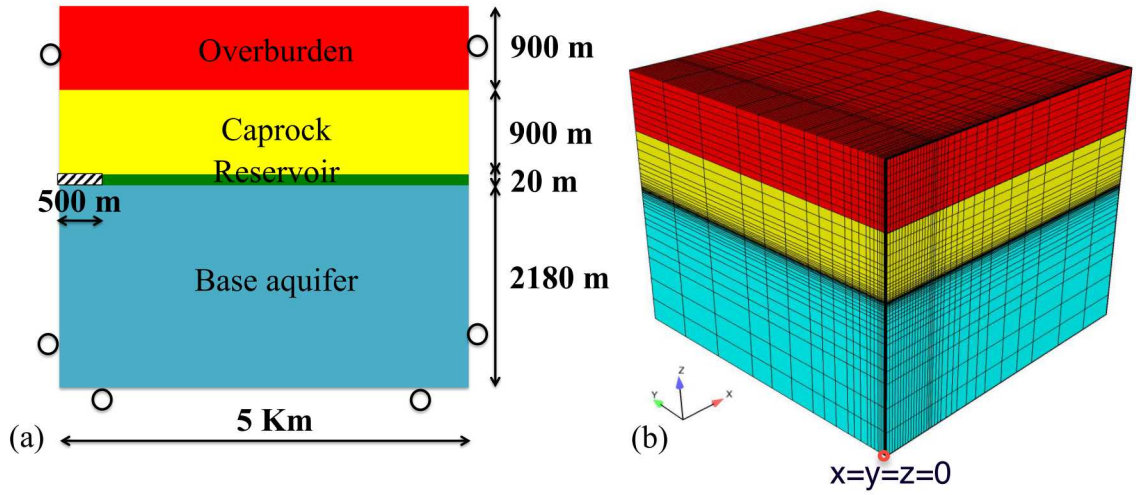

Figure 2: (a) Details of the stratigraphic layers. (b) Schematic of the 3-D domain.

2.2. Coupled flow and geomechanical model

Sierra toolkits developed at Sandia National Laboratories was adopted for the numerical analysis. Sierra is an engineering mechanics simulation code frameworks that includes a suite of highly parallelized finite element analysis modules for different physics (Notz et al., 2007; Martinez et al., 2013). Martinez et al. (Martinez et al., 2013, 2011) provided the details of the numerical modeling of CO_2 injection in GCS systems. Here, we briefly describe the key aspects of coupled multiphase flow and geomechanical model. In this work, Sierra Arpeggio module, which is a coupling module between Aria module for multiphase flow and Adagio module for the solid mechanics was used.

The Aria module uses the mass balance of the two-phase system described as:

$$\begin{aligned} \frac{\delta(\rho_w \phi S_w)}{\delta t} &= \nabla \cdot \left(\rho_w \frac{k_{rw}}{\mu_w} \boldsymbol{K} \cdot (\nabla p - \rho_w \boldsymbol{g}) \right) + Q_w \\ \frac{\delta(\rho_n \phi S_n)}{\delta t} &= \nabla \cdot \left(\rho_n \frac{k_{rw}}{\mu_n} \boldsymbol{K} \cdot (\nabla p_c - \rho_n \boldsymbol{g}) \right) + Q_n \end{aligned} \tag{1}$$

where w and n are describing wetting phase (water) and non-wetting phase (CO_2), respectively. Additionally, ρ is density, ϕ is porosity, S is saturation,

μ is viscosity, $\boldsymbol{K}$ is relative permeability, p_c is capillary pressure defined as: $p_c = p_n - p_w$ and $\boldsymbol{g}$ is gravitation. The pore space is assumed to be fluid saturated: $S_w + S_n = 1$.
The Adagio module assumes the quasi-static formulation of the linear momentum described as:

$$\nabla \cdot \boldsymbol{\sigma} + \rho \boldsymbol{g} = 0 \tag{2}$$

where σ is the Cauchy stress tensor, ρ is bulk density of the mixture and $\boldsymbol{g}$ is gravitation.

The reservoir is initially water-filled and after CO_2 injection, a multiphase flow system can be considered (Vasco and Novali, 2008). For the continuum multiphase flow, supercritical CO_2 and water are treated as two immiscible, compressible phases. For capillary pressure- saturation relationship Van-Genuchten model (Genuchten, 1980) was used and for wetting and non-wetting relative permeabilities Van-Genuchten and cubic functions were employed, respectively. All multiphase flow parameters are the same as used in Rutqvist et al. (Rutqvist et al., 2010). To account for the pore pressure effect on the stress tensor, the poroelasticity theory described as follows was adopted.

$$\boldsymbol{\sigma}^{eff} = \boldsymbol{\sigma} - b\boldsymbol{I}p \tag{3}$$

where $\boldsymbol{\sigma}^{eff}$ is the effective stress tensor, σ is the total stress tensor, b is the Biot's coefficient, $\boldsymbol{I}$ is the identity tensor and p is the pore fluid pressure.

Key hydrogeological and geomechanical properties used in this work are listed in Table 1. Referring to Figure 2, the two adjacent vertical planes, the x-z at y = 0 and the y-z at x = 0 are no-flow boundaries, while their opposite planes at x = 5 km and y = 5 km are under constant pressure corresponding to initial hydrostatic condition. For the solid skeleton, initial lithostatic stress conditions are applied. All vertical sides of the domain are fixed against normal motion. The bottom surface is fixed while the top surface is free to move. Inding and Ringrose (Iding and Ringrose, 2010) reported that the storage unit has the initial temperature ~90°C. Thus, the system was assumed isothermal at 90°C. The average field injection rate was 0.2 megatonne/yr (Mt/ yr) for both KB501 and KB503. It should be noted that the uplift data in this work were obtained graphically from Rutqvist et al. (Rutqvist et al., 2010).

Table 1: Hydrogeological and geomechanical properties of each layer.

Property	**Overburden**	**Caprock**	**Reservoir**	**Base**	**Units**
Vertical intrinsic permeability (k_z)*	1.0×10^{-17}	1.0×10^{-21} 1.0×10^{-19}	1.3×10^{-14}	1.0×10^{-19}	m^2
Anisotropy ratio (a)	1	1	1	1	
Young's modulus (E)	1.5	20	6	20	GPa
Biot's coefficient (b)	1	1	1	1	
Poissons ratio	0.2	0.15	0.2	0.15	
Initial porosity	0.1	0.01	0.17	0.01	
Solid density	2100	2100	2100	2100	kg/m^3

*For the caprock layer, the intrinsic permeability values for KB501 and KB503 regions are 1.0×10^{-21} m^2 and 1.0×10^{-19} m^2, respectively (Rutqvist et al., 2010).

2.3. Systematic parameter variation

Single parameter studies were preformed to observe how the value of each parameter influences the surface uplift. Results of the single parameter study were used to setup initial values for automatic inverse modeling, which will be described in the next section. The measured surface uplift at two injection wells KB501 and KB503 were used to compare simulation results with different parameter values. Since the surface uplift at KB501 is lower than that at KB503, different caprock permeability values were used for KB501 and KB503 (Table 1) based on Rutqvist's suggestion (Rutqvist et al., 2010).

The key parameters investigated include: caprock permeability (k_z), Young's modulus of reservoir and caprock (E_{res} and E_{cap}), Biot's coefficient of reservoir and caprock (b_{res} and b_{cap}), and anisotropy ratio of the reservoir permeability (α_{res}) described as:

$$\alpha = \frac{k_h}{k_v} \tag{4}$$

where k_h is the horizontal intrinsic permeability ($k_x = k_y$) and k_v is the vertical intrinsic permeability (k_z). Caprock permeability for KB501 and KB503 is set to 1.0×10^{-21} m^2 (Sim-KB501) and 1.0×10^{-19} m^2 (Sim- KB503), respectively. For these cases, E_{res} was initially set to 6 GPa as in Rutqvist et al. (Rutqvist et al., 2010). Because of the usage of different E_{res} values in the literature (e.g., (Rutqvist et al., 2010) vs. (Aoyagia et al., 2013) and (Shi et al., 2013)), E_{res} was changed to 10 GPa and subsequently used as a

reference case. Biot's coefficient is a key parameter to couple flow and geomechanical model and it is defined based on Terzaghi's formulation described in Equation 3.

As noted in Table 1, Rutqvist et al. (Rutqvist et al., 2010) suggested two different caprock permeability values to capture the surface uplift of both KB501 and KB503. In order to investigate the possibility of change in other parameters rather than the permeability to capture these surface uplifts, three different cases were studied. In Sim-KB501-Biot, different values of Biot's coefficient (b_{res} = 0.55 and b_{cap} = 0.75) were used. In Sim-KB501-AnisoPerm, $k_z = 1.927\times10^{-14}$ m^2 and α_{res} was set to 0.536. In Sim-KB501-Biot-AnisoPerm, different values of Biot's coefficients (b_{res} = 0.55 and b_{cap} = 0.75), plus anisotropic permeability field for reservoir were used ($k_z = 1.3\times10^{-14}$ m^2 and α_{res} = 0.77). In all these cases, the other parameters remained the same as KB503 and the goal was capturing the surface uplift of KB501.

It should be noted that the maximum change in the pore pressure with respect to the initial pore pressure within the reservoir, due to CO_2 injection (ΔP_{max}) was estimated to be ~10 MPa (Rutqvist et al., 2010). This maximum change in the pore pressure can be supported by bottom hole pressures measured at injection wells (Pamukcu et al., 2011; Shi et al., 2013). Therefore, it is essential to investigate the importance of the constraint on the pore pressure and its impact on the behavior of the overall system.

2.4. Parameter estimation

The parameter estimation package PEST (Doherty, 2011; Doherty and Hunt, 2010) was used to perform model calibration. As described in Table 2, five groups are considered to evaluate the impact of hydrogeological (k_z, α) and geomechanical properties (b, E) of reservoir and caprock on surface uplift and pore pressure increase due to CO_2 injection. Because of limited available observed data, different complexity in parameterization was tested to systematically evaluate the non-uniqueness of parameter estimation. The evaluation was done based on various sets of parameters. Group I calibrates hydrogeological properties (k_z, α) of reservoir. Group II calibrates both hydrogeological and geomechanical properties (k_z, α, b and E) of reservoir. For both groups I and II geomechanical and hydrogeological properties of caprock are prescribed. Group III calibrates both hydrogeological and geomechanical properties (k_z, α, b and E) of caprock using fixed reservoir properties and Group IV calibrates hydrogeological properties ($k_{z,res}$, $k_{z,cap}$, α_{res}, α_{cap}) with

prescribed geomechanical properties (b and E). Group V studies the impact of different combinations of hydrogeological and geomechanical properties for both reservoir and caprock. For both KB501 and KB503, the observed data for model calibration are the maximum surface uplifts over 3 years. Additionally, the maximum pore pressure increase of 10 MPa in the reservoir due to CO_2 injection was included as the observed data ($\Delta P_{max,obs}$ =10 MPa). To evaluate the impact of the inclusion of $\Delta P_{max,obs}$ on the calibration process with the observed uplift data, comparison of model calibration for all five groups with and without $\Delta P_{max,obs}$ was performed.

The total objective function (Φ_{total}) to be minimized is the weighted sum of squared errors between the observed (obs) and simulated (sim) values (m_1) as:

$$\Phi_{total} = \Phi_{uplift} + \Phi_{pressure} = \left(m_1^{obs} - m_1^{sim}\right)^T \boldsymbol{Q} \left(m_1^{obs} - m_1^{sim}\right) \qquad (5)$$

where Φ_{uplift} and $\Phi_{pressure}$ the objective functions from two different observation groups, respectively, diagonal matrix Q represents the square of the weight and a superscript T represents the transpose operation. A weight factor of 0.01 is used for the maximum pressure change, compared to a unit weight factor for all uplift data, to ensure that the objective function values from two different groups (Φ_{uplift} and $\Phi_{pressure}$) are similar. For nonlinear models a parameter upgrade vector is computed from the residual vector and then solved iteratively using the Gauss-Newton method with the Levenberg-Marquardt (LM) parameter (Doherty and Hunt, 2010).

For nonlinear problems, gradient-based local optimization methods are likely to find a set of parameters at the local optimum, which is strongly influenced by the starting value of the estimation (Yoon and McKenna, 2012; Yoon et al., 2013). Hence, multiple sets of parameters may have the same degree of the goodness of fit to the calibration data unless the starting value is close to the best solution, which is unknown for real complex problems. To overcome this issue, a multiple starting approach was evaluated by changing the initial values of estimated parameters. The initial values were selected from the range of possible values for In Salah.

Table 2: Five-parameter groups for model calibration.

Group	**Calibration parameters**
Group I	Permeability parameters for reservoir only ($k_{z,res}$, α_{res})
Group II	Permeability and mechanical parameters for reservoir only ($k_{z,res}$, α_{res}, b_{res}, E_{res}
Group III	Permeability and mechanical parameters for caprock only ($k_{z,cap}$, α_{cap}, b_{cap}, E_{cap})
Group IV	Permeability parameters for both reservoir and caprock ($k_{z,res}$, $k_{z,cap}$, α_{res}, α_{cap})
Group V	Permeability and mechanical parameters for both reservoir and caprock ($k_{z,res}$, $k_{z,cap}$, α_{res}, α_{cap}, b_{cap}, E_{cap})

3. Results and discussions

3.1. Model validation

The base parameters in Table 1 were used in the simulation of In Salah. The simulation results were used to validate our coupled geomechanical, multiphase fluid model. Sim-KB503 used caprock permeability of 1.0×10^{-19} m^2 and Sim-KB501 used 1.0×10^{-21} m^2, as suggested by Rutqvist et al. (Rutqvist et al., 2010). As it was discussed, these simulations are coupled multi-physics in nature and it is not straightforward to decouple the impact of the geomechanical and hydrogeological properties on the surface uplift. However, following Terzaghi's equation (Equation 3), it is clear that the distribution of the pore pressure has an impact on the effective stress field, which influences the strain field following the constitutive laws of each layers. Figure 3 shows how pore pressure affected the vertical total stress field and created the vertical effective stress field based on the Terzaghi's equation. This figure also shows how pore pressure affected the CO_2 saturation field. As a results, the displacement field was affected in the system. One can clearly see, the maximum displacement occurs within the reservoir, where the maximum change in the pore pressure with respect to the initial pore pressure occurs. Moving towards upper layers, the change in the pore pressure decreases and thus the displacement field decreases as well, but most of the surface uplift is due the injection reservoir expansion.

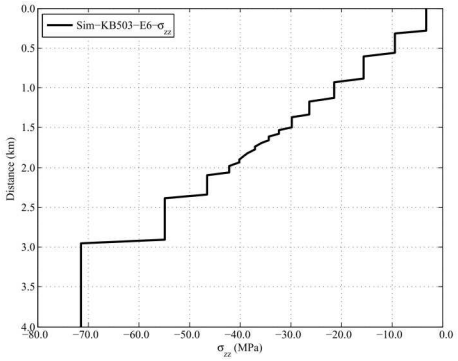

(a) Total vertical stress (σ_{zz}).

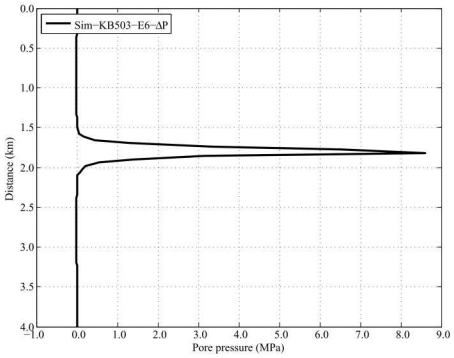

(b) Change in the pore pressure (ΔP).

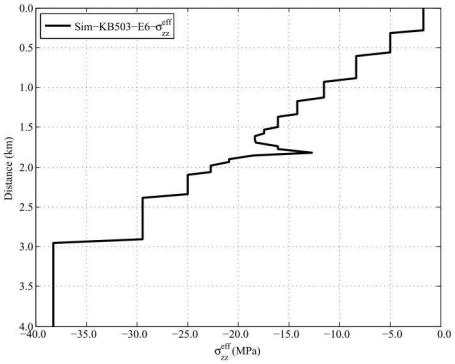

(c) Effective vertical stress (σ_{zz}^{eff}).

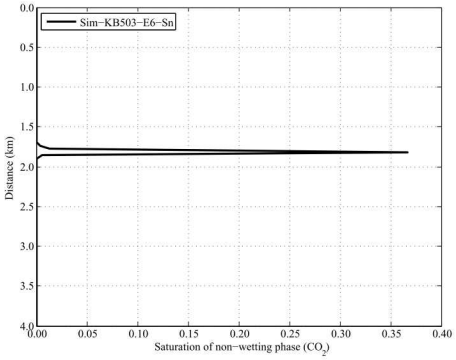

(d) CO_2 saturation (S_n).

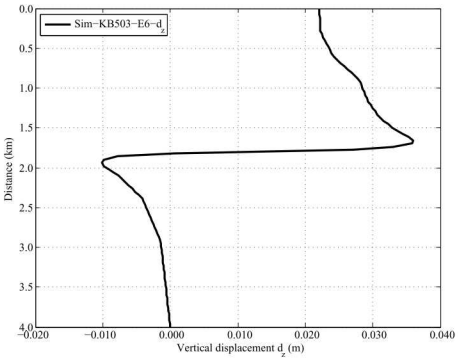

(e) Vertical displacement (d_z).

Figure 3: Details of the impact of each parameter on the surface uplift.

Other works (Aoyagia et al., 2013; Shi et al., 2013) have suggested Young's modulus of 10 GPa for reservoir. Figure 4(a) shows the simulation results for the surface uplift for both KB501 and KB503 using 6 GPa and Figure 4(b) shows results using 10 GPa. One can see, by using 10 GPa for the reservoir, Sim-KB503-E10 and Sim-KB501-E10 match the measured surface uplift evaluated from InSAR data quite well.

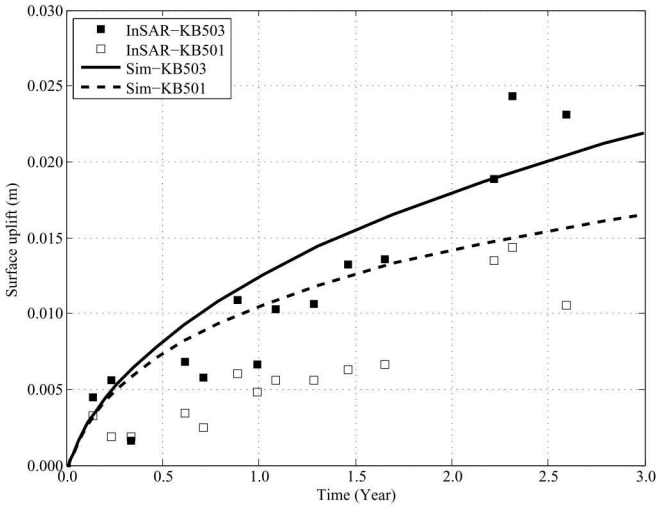

(a)

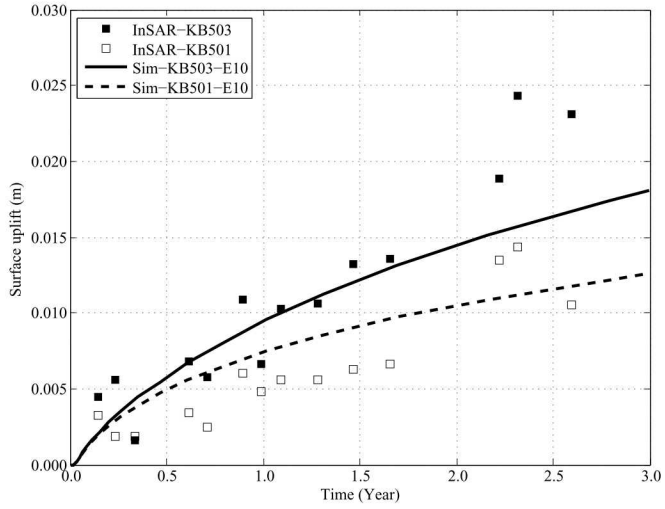

(b)

Figure 4: Comparison of the simulations of the ground surface uplift and the measured data by InSAR: (a) Young's modulus of the reservoir = 6 GPa. (b) Young's modulus of the reservoir = 10 GPa.

The significant impact of Young's modulus on the simulation results demonstrates the need for further investigation on the sensitivity of surface uplift to the other hydrogeological and geomechanical properties. Another field measurement was the maximum change in the pore pressure with respect to the initial pore pressure within the reservoir, which was reported to be ∼10 MPa. Figure 5 shows the maximum pore pressure within the reservoir throughout 3-year simulation period. As it can be seen, the maximum change within the reservoir is ∼9 MPa, which matches the measured data from the field.

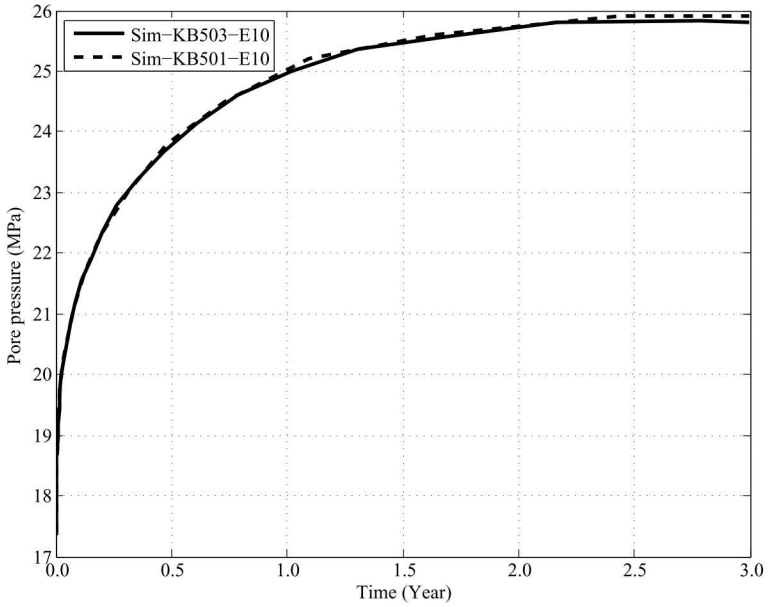

Figure 5: Maximum pore pressure with respect to the initial pore pressure within the reservoir throughout the 3-year simulation for two different simulations: Sim-KB503 is intended to capture the surface uplift of KB503 and Sim-KB501 is intended to capture the surface uplift of KB501.

Figure 6 shows the change in the pore pressure with respect to the initial pore pressure, throughout the depth at year 3. Looking closely at Sim-KB503- E10, where the caprock and base permeabilities are 1.0×10^{-19} m^2, the diffusion of pressure is quite symmetric with respect to the reservoir (between two red lines). However, in Sim-KB501-E10, where the caprock permeability is set to 1.0×10^{-21} m^2, the diffusion of pore pressure is no longer symmetric on both sides of the reservoir. This is mainly due to the fact that the permeability of the base aquifer remained the same (1.0×10^{-19} m^2).

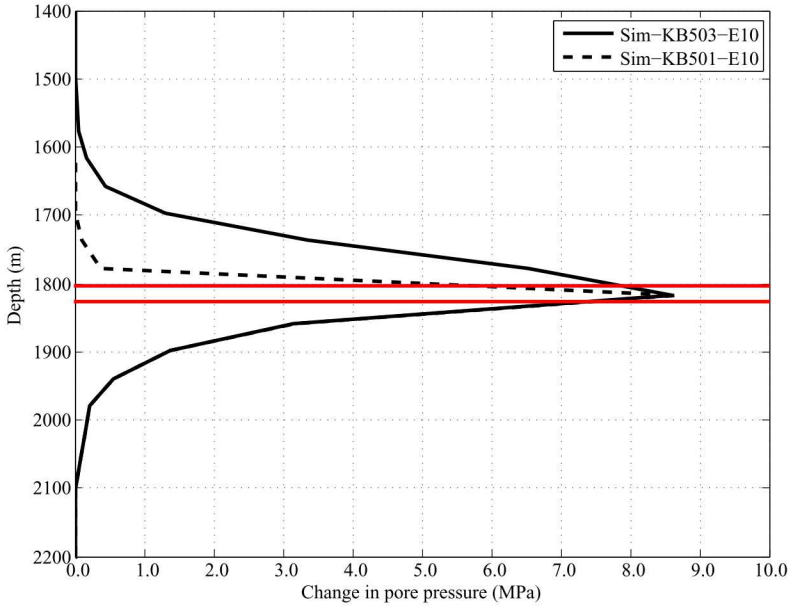

Figure 6: Details of the change in the pore pressure with respect to the initial pore pressure (the reservoir has been defined with two red lines).

It should be noted that multiple levels of refinement were performed on the base mesh for KB503. The refinements were uniform in all directions. The results showed the base mesh (used above) is sufficient to be used for the rest of the study.

A small domain may artificially hold down the injection-induced over pressures in the simulation. Therefore, the domain size was expanded to 15 km in horizontal directions for KB503. Based on the fact that injection takes place in an anticlinal structure, 15 km is about the maximum domain extent without intersecting the gas-water contact. The change in pore pressure throughout the depth of the system at x = 0, x = 2.5 km and x = 5.0 km were compared. Figure 7 shows how the pore pressure is affected by the boundary at these locations after three years of injection. As one can see, there are 34% and 74% increase in the change of the pore pressure at x = 2.5 km and x = 5.0 km at year 3, respectively. However, the maximum change within the reservoir at the symmetry line (x = 0) is not significantly affected by the boundary effect. This shows that the boundary effect is less, closer to the well. Additionally, the overall boundary effect on the pore pressure is less than 1 MPa, when the boundary was extended to 15 km.

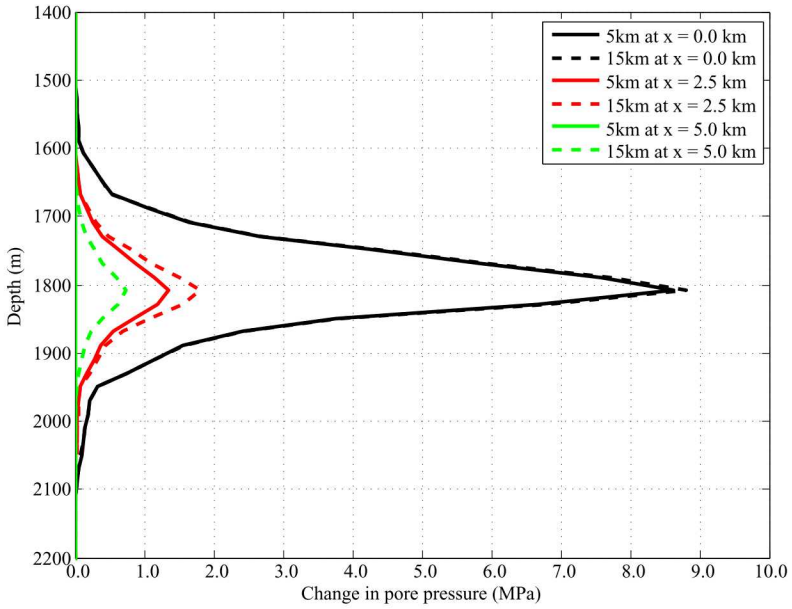

Figure 7: Comparison of the change in the pore pressure for 5 km and 15 km domain at year 3 at three different location x = 0, 2.5 and 5 km.

3.2. Geomechanical and hydrogeological properties

3.2.1. Biot's coefficient at KB501

In order to maximize the effect of the pore pressure on the solid skeleton, it is often assumed that Biot's coefficient of all the layers are equal to one. However, Biot's coefficient of sandstone could be between 0.4-0.6 (Zoback, 2010). Biot's coefficient is expected to change with solid compressibility, so correlation distance would vary on length scales of centimeters to meters. Therefore, it is quite reasonable to assume different Biot's coefficients for different layers of KB501 compared to similar layers in KB503. Havens (Havens, 2012) has shown Biot's coefficient varies from 0.2-0.8 within only 55 meters (2020-2075) depth of the Bakken formation. The authors are aware of the relationship between Biot's coefficient and the Bulk modulus. However, in this study, Biot's coefficient was changed independently from the Bulk modulus of the corresponding layer. As an example, Biot's coefficient of caprock and reservoir were set equal to 0.75 and 0.55, respectively and other parameters remained the same as KB503 (Sim-KB501-Biot). These values were chosen to assure the maximum change in the pore pressure within the reservoir does not surpass 10 MPa. Figure 8 shows the results of the simulations and the impact of the new Biot's coefficients in the surface uplift. As one can see, the new values of the Biot's coefficients can capture the uplift of KB501 quite well. Comparing with Sim-KB501, the initial slope of the curve is such that it even captures the initial uplifts better than the Sim-KB501. Moreover, the maximum change in the pore pressure remains within the observed range ($\sim$9 MPa) and it occurs within the reservoir. In Sim-KB501-Biot, the Biot's coefficient is lower than one, indicating the surface uplift will be lower due to the less impact of the pore pressure on the solid skeleton. This case shows change in Biot's coefficient could be a possible differentiable property between KB501 and KB503.

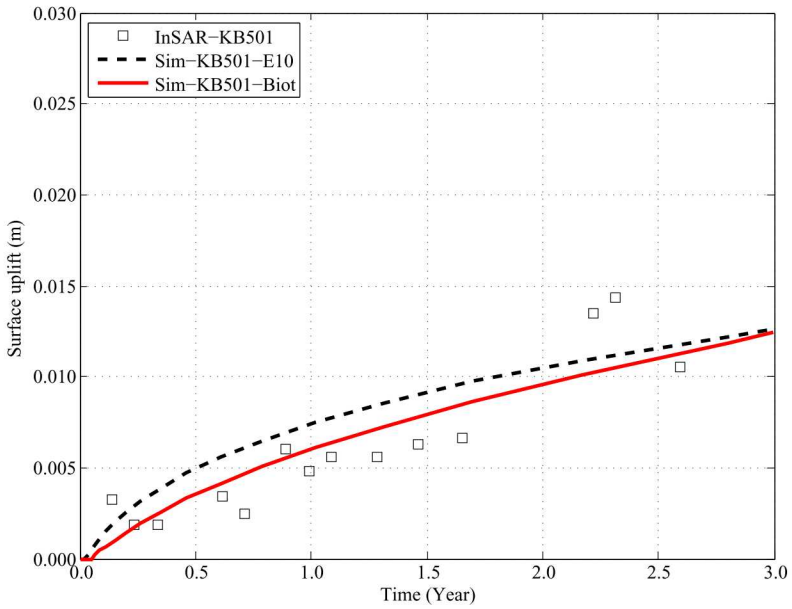

Figure 8: The effect of the Biot's coefficient on the surface uplift inKB501. This case has all the properties of the base case (Sim-KB503-E10), except the Biot's coefficients of reservoir and caprock, which were set equal to 0.75 and 0.55, respectively.

3.2.2. Reservoir's permeability at KB501

Previous researchers (Rutqvist et al., 2010) have chosen an isotropic reservoir permeability, to satisfy the maximum change in the pore pressure. However, Iding and Ringrose (Iding and Ringrose, 2009, 2010) confirmed the nature of pre-existing fractures within the reservoir at In Salah. The image logs of the core data show these fractures are mainly oriented in the near-vertical direction. Therefore, anisotropy in the vertical direction was assumed in the permeability field within the reservoir. In this special case, $k_x = k_y = 1.8\times10^{-14}$ m^2 and $k_z = 0.8\times10^{-14}$ m^2, which implies the anisotropy ratio of 0.536. This is mainly an example to entertain the idea of anisotropic permeability field within the reservoir. Two things were in mind selecting these values: 1) horizontal permeability remains close to 1.4×10^{-14} m^2, and 2) maximum change in the pore pressure with respect to the initial value within the reservoir remains close to 10 MPa. Figure 9 shows the anisotropic permeability can capture the surface uplift of the KB501 reasonably well. This example illustrates the possibility of anisotropic intrinsic permeability field as another option to capture the surface uplift of KB501. Moreover, the maximum change of the permeability remains within the acceptable range ($\sim$9 MPa) and it occurs within the reservoir. It should be noted that in this case, the other parameters remained the same as Sim-KB503.

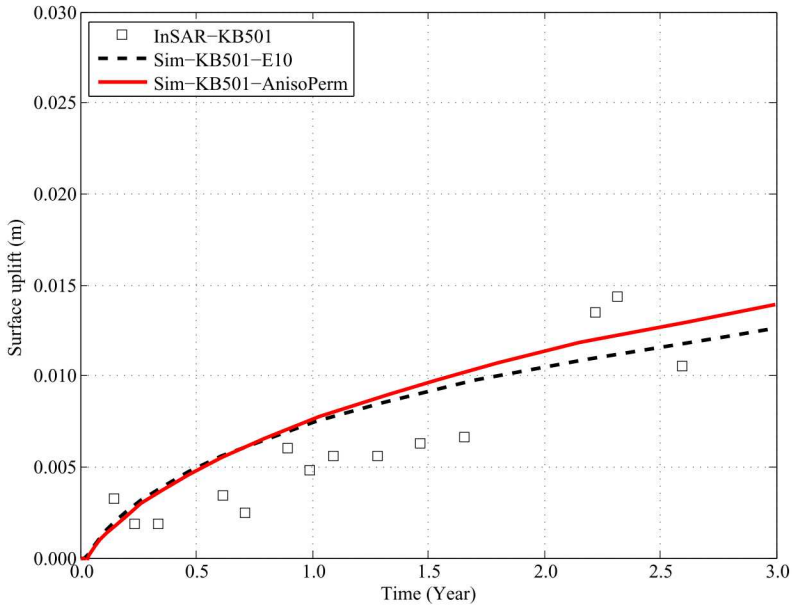

Figure 9: The effect of anisotropic permeability of the reservoir on the surface uplift in KB501. This case has all the properties of the base case (Sim-KB503-E10), except the permeability field for the reservoir, which was defined as: $k_x = k_y = 1.8\times10^{-14}$ m^2 and $k_z = 0.8\times10^{-14}$ m^2. This permeability field implies the anisotropy ratio of 0.536.

3.2.3. Reservoir's permeability at KB503

The possibility of anisotropic permeability field was also tested for KB503. Two different anisotropic permeability fields were tested as listed in Table 3. Horizontal permeabilities were selected to be in the range of 1.0×10^{-14} m^2, to assure the maximum change in the pore pressure within the reservoir is within the acceptable range of the observed data. Figure 10 shows the anisotropy ratio plays an important role in terms of the surface uplifts. Even though, there is an identical surface uplift for both isotropic and anisotropic permeability cases, due to the observed heterogeneity of the rock matrix (Rutqvist et al., 2010; Iding and Ringrose, 2009), the anisotropic permeability field seems more realistic in In Salah field.

Table 3: Different permeability fields for reservoir at KB503.

Case	$\mathbf{k}_x$	$\mathbf{k}_y$	$\mathbf{k}_z$	α
Sim-KB503	1.3×10^{-14}	1.3×10^{-14}	1.3×10^{-14}	1.0
Sim-KB503-AnisoPerm-1	1.033×10^{-14}	1.033×10^{-14}	1.927×10^{-14}	0.54
Sim-KB503-AnisoPerm-2	1.3×10^{-14}	1.3×10^{-14}	2.5×10^{-14}	0.52

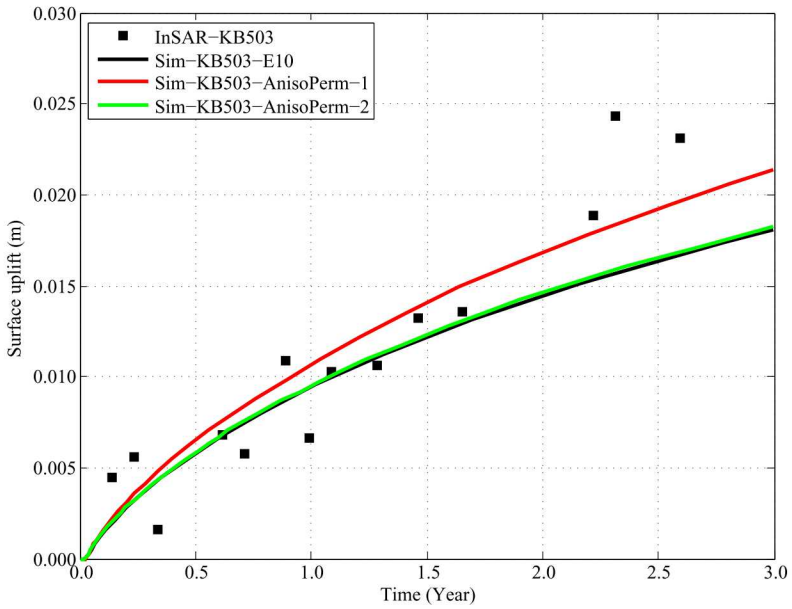

Figure 10: The effect of anisotropic permeability of the reservoir on the surface uplift in KB503. This case has all the properties of the base case (Sim-KB503-E10), except the permeability field for the reservoir, which were defined in Table 3.

3.2.4. Reservoir's permeability and Biot's coefficient at KB501

This case evaluates the combination of the geomechanical (Biot's coefficient) and hydrogeological (anisotropic permeability) properties of reservoir to investigate their impact on the surface uplift. In this case, Biot's coefficient of caprock and reservoir were set to 0.75 and 0.55, respectively. Additionally, $k_x = k_y = 1.0\times10^{-14}$ m^2, $k_z = 1.3\times10^{-14}$ m^2, which implies an anisotropy ratio of 0.77 was used for the reservoir in KB501. This is mainly an example to investigate the impact of combination of the geomechanical and hydrogeological properties different than the properties listed in Table 1 on the surface uplift. Choosing these values was merely based on satisfying the maximum change within the reservoir to remain within the observed data. Figure 11 shows the result of this example case. As one can see, the new properties capture the evaluated uplift data from InSAR reasonably well.

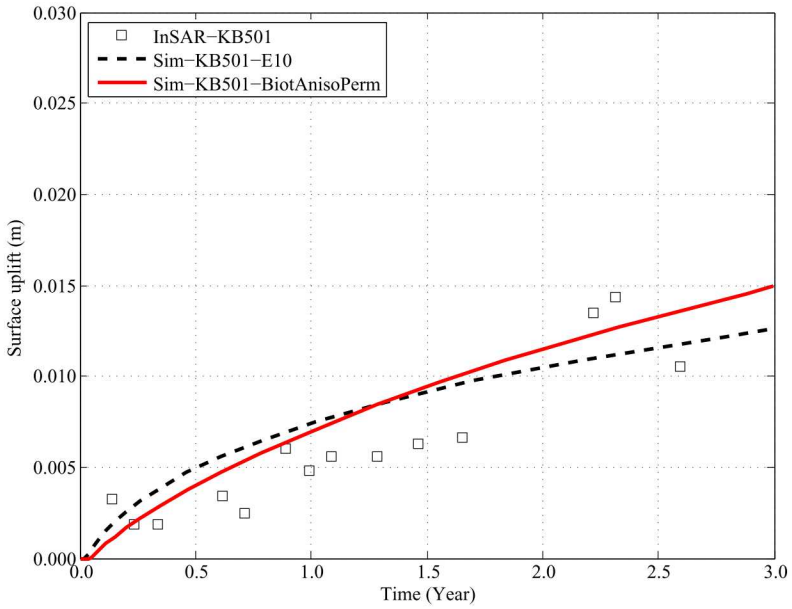

Figure 11: The effect of combination of the geomechanical (Biot's coefficient) and hydrogeological (anisotropic permeability) properties of reservoir on the surface uplift in KB501. This case has all the properties of the base case (Sim-KB503-E10), except the permeability field for the reservoir, which was defined as: $k_x = k_y = 1.0\times10^{-14}$ m^2, $k_z = 1.3\times10^{-14}$ m^2 and the Biot's coefficient of caprock and reservoir, which were set to 0.75 and 0.55, respectively.

The foregoing parameter studies illustrated that the InSAR data can be fit

equally well by variation of different sets of hydogeological or geomecahnical properties or both. The next section uses parameter estimation techniques to better constrain these properties.

3.3. Parameter estimation

Four key parameters (k_z, α, b, and E) for reservoir (res) and caprock (cap) layers were estimated against the observed surface uplift data at KB501 and KB503, and the maximum change in the pore pressure (∼10 MPa). As described in Table 2, five different parameter groups are chosen to evaluate the impact of hydrogeological and geomechanical properties as well as the inclusion of $\Delta P_{max,obs}$ on parameter estimation. Since multiple sets of parameters are expected to match the set of observed data equally likely, it is important to evaluate the significance of different sets of parameters on model calibration. In Tables 4 and 5, the maximum change in the pore pressure (ΔP_{max}) was computed with calibrated parameter values. The final values of estimated parameters were selected when the value of the uplift objective function (Φ_{uplift}) converged to less than 10^{-4}, except in Group III for KB503, which had a bad convergence. The estimated parameters are presented as gray-shaded values in Tables 4 and 5.

3.3.1. Low uplift at KB501

Depending on the initial values and a set of estimated parameters, the k_z value of the caprock ($k_{z,cap}$) ranged from 10^{-21} to 10^{-19} m^2. The k_z value of the reservoir ($k_{z,res}$) has a narrow range around a reference value of 1.3×10^{-14} m^2 except in Group I. For all cases in Groups I-IV, the horizontal permeability of the reservoir ($k_{z,res} \times \alpha_{res}$) are very similar to the reference value, while $k_{z,cap}$ values are low to match the low uplift at KB501. This indicates that lower $k_{z,res}$ values with ΔP_{max} constraint were compensated by higher α_{res} values to dissipate the pore pressure increase from the injection zone to match the low uplift under the low caprock permeability during model calibration. However, KB501-4 (Group II) and cases in Group V show lower α_{res} values and particularly, KB501-4 and10 with ΔP_{max} constraint have lower Biot's coefficients. As discussed in the previous section, the Biot's coefficient and pore pressure increase are inter-related through the effective stress. The lower Biot's coefficient and higher vertical permeability have an opposite effect on the maximum uplift. KB501-10 clearly shows that the positive impact of higher $k_{z,cap}$ and lower α_{res} on uplift was reduced by the negative impact of lower b_{cap} value on uplift, matching the low uplift very well

(Table 4 and Figure 12). This is also supported by the negative correlation coefficient (-0.90) between $k_{z,cap}$ and b_{cap}. In addition, higher variance values for $k_{z,cap}$ (43.5) and α_{cap} (3.95) than those for $k_{z,res}$ (5.03) and α_{res} (0.84) indicates that caprock hydrogeological parameters are less constrained to the observed data than reservoir properties.

All cases for KB-501 match the surface uplift relatively well both in terms of Φ_{uplift} (Table 4) and through visual comparison (Figure 12), confirming that multiple sets of parameters can match the observed data well. However, comparison of model calibration with and without ΔP_{max} constraint shows that ΔP_{max} values computed using calibrated parameters without the constraint are much lower than those with the constraint. For example, Groups II (cases 4 and 5) and V (cases 10 and 12) show that with the pore pressure constraint both Biot's coefficient and anisotropy ratio parameters are calibrated differently, reconfirming that the inclusion of the pore pressure data is critically important to constrain the parameter solution direction during model calibration. As demonstrated in Figure 11, both geomechanical (b_{res}) and hydrogeological (α_{res}) parameters play a key role in the pore pressure propagation through reservoir and the magnitude of the surface uplift. Therefore, parameter estimation results highlight the significance of coupled impact of hydrogeological and geomechanical properties during GCS. With ΔP_{max} constraint Young's modulus are very close to the base value for all layers, indicating the base values of Young's modulus may represent the geomechanical properties well.

Table 4: Calibration results for KB-501 cases.

Group	Group I			Group II		Group III		Group IV		Group V		
Case	1	2	3	4	5	6	7	8	9	10	11	12
Calibrated Model Parameter Values												
kz_cap (m^2)	$1.00E^{-20}$	$1.00E^{-21}$	$1.00E^{-20}$	$1.00E^{-20}$	$1.00E^{-20}$	$5.07E^{-21}$	$2.29E^{-21}$	$2.38E^{-21}$	$4.47E^{-20}$	$9.15E^{-20}$	$1.06E^{-19}$	$8.12E^{-20}$
kz_res (m^2)	$3.34E^{-15}$	$1.68E^{-15}$	$1.61E^{-14}$	$2.39E^{-14}$	$1.14E^{-14}$	$1.75E^{-14}$	$1.30E^{-14}$	$1.75E^{-14}$	$4.27E^{-14}$	$1.59E^{-14}$	$2.06E^{-14}$	$1.51E^{-14}$
α_{cap}	1.000	1.000	1.0000	1.0000	1.0000	0.458	0.516	0.869	1.452	0.972	1.219	1.024
α_{res}	4.274	8.543	1.036	0.429	1.158	1.000	1.000	1.000	0.547	0.67	0.481	1.095
b_{cap}	1.000	1.000	1.000	1.000	1.000	1.000	1.000	1.000	1.000	0.644	0.6	0.681
b_{res}	1.000	1.000	1.000	0.525	1.000	0.55	0.550	1.000	1.000	0.550	0.550	1.000
E_{cap} (GPa)	20	20	20	20	20	17.8	17.8	20	20	20	20	20
E_{res} (GPa)	10	10	10	9.76	9.84	10	10	10	10	10	10	10
Computed Results ⋆												
ΔP_{max} †	9.18	9.44	6.94	9.94	8.8	6.58	8.8	6.58	4.54	9.99	10.3	7
Φ_{uplift}	$7.32E^{-05}$	$6.97E^{-05}$	$6.43E^{-05}$	$5.44E^{-05}$	$9.03E^{-05}$	$9.12E^{-05}$	$5.41E^{-05}$	$7.15E^{-05}$	$7.10E^{-05}$	$4.54E^{-05}$	$4.51E^{-05}$	$6.00E^{-05}$
$\Phi_{pressure}$	$6.77E^{-05}$	$3.16E^{-05}$	n.a.	$1.90E^{-05}$	n.a.	$1.17E^{-03}$	$1.45E^{-05}$	$1.17E^{-03}$	n.a.	$1.40E^{-08}$	n.a.	n.a.
Φ_{total}	$1.41E^{-05}$	$1.01E^{-04}$	$6.43E^{-05}$	$7.34E^{-05}$	$9.03E^{-05}$	$1.26E^{-03}$	$1.99E^{-04}$	$1.24E^{-03}$	$7.10E^{-05}$	$4.54E^{-05}$	$4.51E^{-05}$	$6.00E^{-05}$

Highlighted parameters in gray are estimated with other parameters fixed.
Cases without pressure constraint show no objective function value as indicated by n.a..
⋆Final estimated values are the same as the initial values of parameters.
†ΔP_{max} is the computed maximum pore pressure change (in MPa) with calibrated parameter values.

3.3.2. High uplift at KB503

In contrast to the KB501 cases, the surface uplift in KB503 was high, estimating high $k_{z,cap}$ (all cases except case 11), high Biot's coefficient (Groups II and V), and/or low Young's modulus (cases 10 and 11). As in the KB501 cases, all cases match the surface uplift well (Table 5 and Figure 12). For all starting values and different sets of parameters, $k_{z,res}$ has a very narrow range of estimated values close to the reference value (1.3×10^{-14} m^2). As shown in Figure 5, the pore pressure corresponding to the high surface uplift at KB503 propagates significantly in the caprock layer. This indicates reservoir and caprock properties at KB503 might be more inter-related. For example, compared to correlations between hydrogeological and geomechanical parameters for the KB501-10 (e.g., -0.2 for α_{res}-b_{cap} and 0.24 for $k_{z,res}$-b_{cap}), the KB503-10 case has higher correlations (e.g., -0.89 for α_{res}-b_{cap} and 0.91 for $k_{z,res}$-b_{cap}).

The importance of multiple observed data is also shown by computed ΔP_{max} values. Without the pore pressure constraint, computed ΔP_{max} values were higher for all cases in KB503 than in KB501. It should be noted that the surface uplift tends to calibrate the model without direct information regarding the pressure propagation or CO_2 plume development. This strongly suggests that calibration of both hydrogeological and geomechanical properties together with multiple datasets can constrain parameter space closer to actual physical setting.

Table 5: Calibration results for KB-503 cases.

Group	Group I			Group II		Group III		Group IV		Group V		
Case	1	2	3	4	5	6	7	8	9	10	11	12
Calibrated Model Parameter Values												
kz_cap (m^2)	$1.00E^{-19}$	$1.00E^{-19}$	$1.00E^{-19}$	$1.00E^{-19}$	$1.00E^{-19}$	$4.57E^{-20}$	$1.45E^{-19}$	$1.72E^{-19}$	$2.77E^{-20}$	$1.29E^{-19}$	$1.20E^{-19}$	$1.39E^{-19}$
kz_res (m^2)	$2.03E^{-14}$	$1.93E^{-14}$	$1.08E^{-14}$	$4.09E^{-14}$	$1.33E^{-14}$	$1.30E^{-14}$	$3.16E^{-14}$	$1.02E^{-14}$	$8.68E^{-15}$	$2.26E^{-14}$	$1.58E^{-14}$	$1.97E^{-14}$
α_{cap}	1.000	1.000	1.000	1.000	1.000	0.844	0.750	0.311	0.250	1.015	1.485	1.715
α_{res}	0.511	0.536	0.895	0.225	0.623	1.000	1.000	1.079	0.872	0.431	0.644	0.283
b_{cap}	1.000	1.000	1.000	1.000	1.000	0.986	0.750	1.000	1.000	1.000	1.000	0.862
b_{res}	1.000	1.000	1.000	0.879	0.779	0.550	0.550	1.000	1.000	0.550	0.550	0.550
E_{cap} (GPa)	20	20	20	20	20	17.8	18.6	20	20	17.8	17.8	20.9
E_{res} (GPa)	10	10	10	9.83	10.85	10	10	10	10	10	10	10
Computed Results												
ΔP_{max} †	10.02	10.10	11.30	10.03	12.50	8.75	6.57	10.31	14.08	10.3	10.4	16.2
Φ_{uplift}	$9.93E^{-05}$	$9.92E^{-05}$	$9.47E^{-05}$	$8.96E^{-05}$	$8.25E^{-05}$	$3.54E^{-05}$	$1.80E^{-05}$	$9.79E^{-05}$	$9.68E^{-05}$	$7.98E^{-05}$	$9.29E^{-05}$	$7.10E^{-05}$
$\Phi_{pressure}$	$4.00E^{-08}$	n.a	n.a.	$9.00E^{-08}$	n.a.	$1.55E^{-04}$	$1.18E^{-03}$	$9.61E^{-06}$	n.a.	$1.09E^{-05}$	$1.85E^{-05}$	n.a.
Φ_{total}	$17.10E^{-05}$	$9.92E^{-05}$	$9.47E^{-05}$	$8.96E^{-05}$	$8.25E^{-05}$	$5.09E^{-04}$	$1.36E^{-03}$	$9.03E^{-05}$	$9.68E^{-05}$	$9.07E^{-05}$	$1.11E^{-05}$	$7.10E^{-05}$

Highlighted parameters in gray are estimated with other parameters fixed.
Cases without pressure constraint show no objective function value as indicated by n.a..
$^{\dagger}\Delta P_{max}$ is the computed maximum pore pressure change (in MPa) with calibrated parameter values.

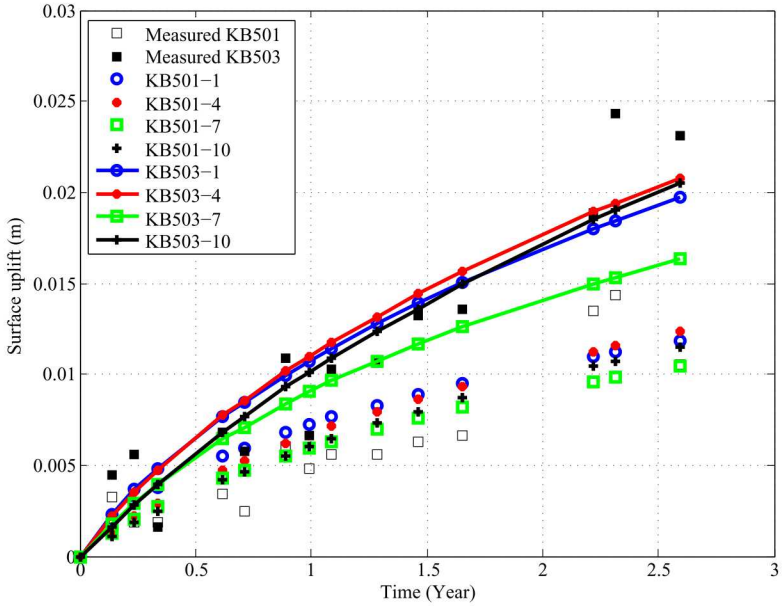

Figure 12: Comparison of observed and modeled uplifts for KB501 (symbol only) and KB503 (symbol + line) with different calibrated sets of parameters. Estimated parameters are presented in Table 4 and 5.

3.3.3. Implications for practical applications

Pamukcu et al. (Pamukcu et al., 2011) calibrated the dual porosity and permeability model by trail-and-error against the bottom hole pressure and the CO_2 breakthrough time. The model parameters consist of permeabilities of reservoir and overlying lower caprock layers. Their manual sensitivity results show that the reservoir has a higher anisotropy ratio (i.e, higher horizontal permeability) from 10 to 100 for matrix and fracture, respectively. In this work, it was found that high α_{res} values can be obtained with reservoir hydrogeological parameters (Group I in KB501) and a lower E_{res} of 6 GPa (results not shown), which is lower than actual value of 10 GPa. The high α_{res} reported in Pamukcu et al. (Pamukcu et al., 2011) may result from an incomplete set of model parameters and/or an improper value of geomechanical parameters. In contrast, our results indicate that with a proper E_{res} value ($\sim$10 GPa) automatic calibration results with the surface uplift data and pore pressure data may reflect an average value of matrix and fracture permeability.

At In Salah, the site characterization based on one injection well has been applied for characterizing hydrogeological features around other injection wells (Shi et al., 2012, 2013). Based on cross-validation and analysis of variance methods with 13 input parameters for coupled multiphase flow and geomechanical simulations with varying injection rate in a 2D layered system with a 200 m of reservoir layer and a 100 m of caprock layer, Bao et al. (Bao et al., 2013) concluded the three most significant parameters to surface uplift and pore pressure increase are reservoir porosity, permeability, and injection rate. Caprock properties are generally less significant than reservoir properties. In this work, however, caprock properties are very important to match the surface uplift with pore pressure constraint. This difference can be attributed to the thickness of reservoir and caprock, which results in different sensitivity of parameters to surface uplift and pore pressure distribution. Overall, comparison of low and high uplift cases in this work suggests that one should be cautious with site characterization or determining operation conditions, since parameter correlations and/or their sensitivity to observed data can vary even at the same site as shown in this case.

As expected for strong nonlinear problems, model calibration was significantly influenced by the starting values. For example, the high surface uplift coupled with the maximum pore pressure constraint results in very narrow solution space and lower caprock permeability as a starting point results in poor convergence. Overall, calibration results with different starting parameters and different calibration groups provide a range of estimated parameters matching both observed data. Recently, Ringrose et al. (Ringrose et al., 2013) summarized the key elements of site characterizations and monitoring technologies applied at In Salah site, highlighting the significance of integrated approach to the development of monitoring, modeling and verification (MMV) for CO_2 storage. As suggested by Ringrose et al., this work also supports that calibration of coupled reservoir and geomechanics model integrated with geophysical characterization techniques will provide a practically efficient tool for developing actual operations of CO_2 injection and monitoring/evaluating its associated risk assessments.

4. Conclusions

This study revealed that the coupled hydromechanical process plays an important role in determining CO_2 activity and it is quite essential to measure geomechnaical and hydrogeological properties of each layer to have a better

understanding of the GCS system. Additionally, it is important to realize that the formation inflation, leading to the surface uplift, is impacted by the caprock and base permeabilities via diffusion of pressure from the injection zone even though the injected CO_2 is contained in the injection interval. To the best knowledge of the authors, this is the only study looking at the effect of Biot's coefficient and anisotropy ratio on the surface uplift at In Salah, KB501 and KB503. Pore pressure constraint is another unique factor of this article being investigated in terms of surface uplift in both KB501 and KB503. However, this study did not account for heterogeneity in rock layers. Overall, this study shows:

(1) Geomechanical and hydrogeological properties are equally important to understanding the surface uplift at In Salah.
(2) Various combinations of geomechanical and hydrogeological properties can fit the known data equally well.
(3) The base vertical intrinsic permeability and Young's modulus of the reservoir remained close to 10-14 mD (1.0×10^{-14}-1.4×10^{-14} m^2) and 10 GPa, respectively. This indicated the robustness of these parameters over many variations of other parameters in order to satisfy the pore pressure constraint.
(4) Some of the cases in parameter estimation of reservoir permeability suggest consistency with the fracturing suggested by Ringrose et al. (Ringrose et al., 2013).
(5) The pore pressure constraint is a key factor in parameter estimation.

Acknowledgments

This work is supported as part of the Center for Frontiers of Subsurface Energy Security, an Energy Frontier Research Center funded by the U.S. Department of Energy, Office of Science, Office of Basic Energy Sciences under Award Number DE-SC0001114. Sandia National Laboratories is a multi-program laboratory managed and operated by Sandia Corporation, a wholly owned subsidiary of Lockheed Martin Corporation, for the U.S. Department of Energy's National Nuclear Security Administration under contract DE-AC04-94AL85000.

Aoyagia, R., Imai, R., Rutqvist, J., Kobayashi, H., Kitamura, O., Goto, N., 2013. Development of TOUGH-FrontISTR, a numerical simulator for environmental impact assessment of CO_2 geological storage. Energy Procedia 37, 3655 – 3662, 11^{th} International Conference on Greenhouse Gas Control Technologies.

Bao, J., Hou, Z., Fang, Y., Ren, H., Lin, G., 2013. Uncertainty quantification for evaluating impacts of caprock and reservoir properties on pressure buildup and ground surface displacement during geological co2 sequestration. Greenhouse Gases: Science and Technology 3 (5), 338 – 358.

Deflandre, J., Estublier, A., Baroni, A., Daniel, J., Adjmian, F., 2011. In Salah CO_2 injection modeling: A preliminary approach to predict short term reservoir behavior. Energy Procedia 4 (0), 3574 – 3581, 10^{th} International Conference on Greenhouse Gas Control Technologies.

Doherty, J., 2011. PEST: Model independent parameter estimation.

Doherty, J., Hunt, R. J., 2010. Approaches to highly parameterized inversion: A guide to using pest for groundwater-model calibration.

Eiken, O., Ringrose, P., Hermanrud, C., Nazarian, B., Torp, T. A., Hier, L., 2011. Lessons learned from 14 years of CCS operations: Sleipner, in salah and snhvit. Energy Procedia 4 (0), 5541 – 5548, 10^{th} International Conference on Greenhouse Gas Control Technologies.

Espinet, A. J., Shoemaker, C. A., 2013. Comparison of optimization algorithms for parameter estimation of multi-phase flow models with application to geological carbon sequestration. Advances in Water Resources 54 (0), 133 – 148.

Genuchten, M. T. V., 1980. A closed-form equation for predicting the hydraulic conductivity of unsaturated soils. Soil science society of America journal 44 (5), 892 – 898.

Havens, J., 2012. Mechanical properties of the bakken formation. Master's thesis, Colorado school of Mines.

Iding, M., Ringrose, P., 2009. Evaluating the impact of fractures on the long-term performance of the In Salah CO_2 storage site. Energy Procedia 1 (1), 2021 – 2028.

Iding, M., Ringrose, P., 2010. Evaluating the impact of fractures on the performance of the In Salah CO_2 storage site. International Journal of Greenhouse Gas Control 4 (2), 242 – 248.

Martinez, M., Newell, P., Bishop, J., Turner, D., 2013. Coupled multiphase flow and geomechanics model for analysis of joint reactivation during CO_2 sequestration operations. International Journal of Greenhouse Gas Control 17, 148 – 160.

Martinez, M. J., Stone, M. C., Notz, P. K., Tuner, D. Z., Hopkins, P. L., Subia, S., Jove-Colon, C., Moffat, H. K., Bean, J. E., Dewers, T., Klise, K., Red-Horse, J., R, R. F., Mesh, M., Davison, S., Yoon, H., Carnes, B., Alger, N., Bishop, J. E., Newell, P., 2011. Computational thermal, chemical, fluid and solid mechanics for geosystems management. SAND2011-6643.

McKenna, S. A., Pike, D. Q., 2013. Fluid pressure redistribution events within a fault: impact of material property correlation.

Nanayakkara, A. S., Wong, R. K., 2009. How far does surface heave propagate? a discussion on analytical and numerical modeling of the surface heave induced by subsurface fluid injection. KSCE Journal of Civil Engineering 13 (4), 297 – 303.

Notz, P., Subia, S., Hopkins, M., Moffat, H., Noble, D., 2007. Aria 1.5: User manual. SAND2007-2734.

Pamukcu, Y., Hurter, S., Jammes, L., Vu-Hoang, D., Pekot, L., 2011. Characterizing and predicting short term performance for the In Salah krechba field CCS joint industry project. Energy Procedia 4 (0), 3371 – 3378, 10^{th} International Conference on Greenhouse Gas Control Technologies.

Preisig, M., Prevost, J. H., 2011. Coupled multi-phase thermo-poromechanical effects. case study: CO_2 injection at In Salah, Algeria. International Journal of Greenhouse Gas Control 5 (4), 1055 – 1064.

Ringrose, P., Mathieson, A., Wright, I., Selama, F., Hansen, O., Bissell, R., Saoula, N., Midgley, J., 2013. The in salah co_2 storage project: Lessons learned and knowledge transfer. Energy Procedia 37 (0), 6226 – 6236, 11^{th} International Conference on Greenhouse Gas Control Technologies.

Rutqvist, J., Vasco, D. W., Myer, L., 2009. Coupled reservoir-geomechanical analysis of CO_2 injection at In Salah, Algeria. Energy Procedia 1 (1), 1847 – 1854.

Rutqvist, J., Vasco, D. W., Myer, L., 2010. Coupled reservoir-geomechanical analysis of CO_2 injection and ground deformations at In Salah, Algeria. International Journal of Greenhouse Gas Control 4 (2), 225 – 230.

Shi, J., Sinayuc, C., Durucan, S., Korre, A., 2012. Assessment of carbon dioxide plume behaviour within the storage reservoir and the lower caprock around the kb-502 injection well at in salah. International Journal of Greenhouse Gas Control 7 (0), 115 – 126.

Shi, J., Smith, J., Durucan, S., Korre, A., 2013. A coupled reservoir simulation-geomechanical modelling study of the CO_2 injection-induced ground surface uplift observed at krechba, In Salah. Energy Procedia 37 (0), 3719 – 3726.

Smith, J., Durucan, S., Korre, A., Shi, J., 2013. A methodology to assess increased storage capacity provided by fracture networks at CO_2 storage sites: Application to In Salah storage site. Energy Procedia 37 (0), 3711 – 3718.

Smith, J., Durucan, S., Korre, A., Shi, J., Sinayuc, C., 2011. Assessment of fracture connectivity and potential for CO_2 migration through the reservoir and lower caprock at the In Salah storage site. Energy Procedia 4 (0), 5299 – 5305, 10^{th} International Conference on Greenhouse Gas Control Technologies.

Tavakoli, R., Yoon, H., Delshad, M., ElSheikh, A. H., Wheeler, M. F., Arnold, B. W., 2013. Comparison of ensemble filtering algorithms and null-space monte carlo for parameter estimation and uncertainty quantification using CO_2 sequestration data. Water Resources Research 49 (12), 8108 – 8127.

Vasco, D., Ferretti, A., Novali, F., 2008. Estimating permeability from quasi-static deformation: Temporal variations and arrival time inversion. Geophysics 73 (6), O37 – O52.

Vasco, D. W., Novali, A. F., 2008. Reservoir monitoring and characterization using satellite geodetic data: Interferometric synthetic aperture radar

observations from the krechba field, Algeria. Geophysics 73 (6), WA113 – WA122.

Vasco, D. W., Rucci, A., Ferretti, A., Novali, F., Bissell, R. C., Ringrose, P. S., Mathieson, A. S., Wright, I. W., 2010. Satellite-based measurements of surface deformation reveal fluid flow associated with the geological storage of carbon dioxide. Geophysical Research Letters 37 (3).

Verdon, J. P., Kendall, J. M., Stork, A. L., Chadwick, R. A., White, D. J., Bissell, R. C., 2013. Comparison of geomechanical deformation induced by megatonne-scale CO_2 storage at sleipner, weyburn, and in salah (supplement).

Wainwright, H. M., Finsterle, S., Zhou, Q., Birkholzer, J. T., 2013. Modeling the performance of large-scale CO_2 storage systems: A comparison of different sensitivity analysis methods. International Journal of Greenhouse Gas Control 17 (0), 189 – 205.

Yoon, H., Hart, D. B., McKenna, S. A., 2013. Parameter estimation and predictive uncertainty in stochastic inverse modeling of groundwater flow: Comparing null-space monte carlo and multiple starting point methods. Water Resources Research 49 (1), 536 – 553.

Yoon, H., McKenna, S. A., 2012. Highly parameterized inverse estimation of hydraulic conductivity and porosity in a three-dimensional, heterogeneous transport experiment. Water Resources Research 48 (10), W51036:1 – 17.

Zoback, M. D., 2010. Reservoir geomechanics. Cambridge University Press.